Lawrence Berkeley National Laboratory

Title
Characterization and Electrochemical Performance of Substituted LiNi0.4Co0.2-yAlyMn0.4O2 (0<_y<_0.2) Cathode Materials

Permalink

Author
Wilcox, James D.

Publication Date
2008-11-26

Characterization and Electrochemical Performance of Substituted $LiNi_{0.4}Co_{0.2-y}Al_yMn_{0.4}O_2$ (0≤y≤0.2) Cathode Materials

J. D. Wilcox[a,b] and M. M. Doeff[a]

[a]Materials Sciences Division, Lawrence Berkeley National Laboratory, University of California Berkeley, Berkeley, California 94720, USA
[b]Department of Material Science and Engineering, University of California Berkeley, Berkeley, California 94720, USA

A complete series of $LiNi_{0.4}Co_{0.2-y}Al_yMn_{0.4}O_2$ (0≤y≤0.2) materials have been synthesized and investigated as cathode materials for lithium ion batteries. When cycled between 2.0 and 4.3 V vs. Li/Li^+ at a current density of 0.1 mA/cm^2, stable capacities of ~160 mAh/g for y=0 to ~110 mAh/g for y=0.2 are achieved. Upon increasing the current density, it is found that all materials containing aluminum show reduced polarization and improved rate performance. The optimal performance at all current densities was found for the compound with y=0.05. The effect of aluminum substitution on the crystal structure of the host is discussed.

Introduction

The restricted practical capacity (140 mAh/g), toxicity concerns, and high material costs of $LiCoO_2$ used in the current generation of lithium ion batteries have prompted development of alternative layered oxide cathode materials. Ternary mixed transition metal oxides containing varying amounts of cobalt, nickel, and manganese, such as $LiNi_{1/3}Co_{1/3}Mn_{1/3}O_2$, have been the focus of intense investigation (1,2). These compounds crystallize with the α-$NaFeO_2$ structure (O3 in layered notation, space group R-3m), similar to $LiCoO_2$, but generally have higher practical capacities. Of particular interest is $LiNi_{0.4}Co_{0.2}Mn_{0.4}O_2$ because of its low cobalt content and the high reversible capacity of ~180 mAh/g when cycled to 4.3 V versus lithium (3).

Substitution of transition metal oxides with aluminum has also been studied in the literature. It has been found that α-$LiAlO_2$ is isostructural with $LiCoO_2$, but above 600° C it transforms to the γ-$LiAlO_2$ phase with the γ-$NaFeO_2$ structure, space group 4_12_12 (4). During transformation, the aluminum ions convert from octahedral to tetrahedral coordination. However, it is possible to find stable $Li(Al,M)O_2$ (where M is a transition metal) solid solutions at higher temperatures due to entropically driven mixing, but there is decreasing solubility at higher temperatures (5). The extraction of lithium from α-$LiAlO_2$ has even been predicted to be feasible from first principle methods (6) at voltages approaching 5.4 V versus Li/Li^+ although it is not expected to be reversible.

The substitution of aluminum into $LiNiO_2$ has been shown to decrease the amount of cation mixing (7) and improve the reversibility of the reaction. This is due either to the suppression of the two phase reaction at high states of charge (8), stabilization by prevention of full lithium removal (9), or to the formation of an insulating phase that prevents overcharge (10,11).

The purpose of this study was to determine the effect of Al substitution on the electrochemical performance of mixed transition metal oxides, with a goal of reducing

the cobalt content further. Because most of the Co is not redox active until high potentials vs. Li are reached, it is possible that partial or full replacement with electrochemically inactive Al will have minimal impact on the capacity under normal cycling conditions. Because of the excellent electrochemical properties of the end-member $LiNi_{0.4}Co_{0.2}Mn_{0.4}O_2$ and the possibility of full replacement of Co with Al, the $LiNi_{0.4}Co_{0.2-y}Al_yMn_{0.4}O_2$ ($0{\leq}y{\leq}0.2$) system was selected.

Experimental

All materials were synthesized using the glycine nitrate combustion process ([12]). Stoichiometric mixtures of $LiNO_3$ (Mallinckrodt), $Mn(NO_3)_2$ (45-50 wt.% in dilute nitric acid, Sigma Aldrich), $Co(NO_3)_2$-$6H_2O$ (98%, Sigma Aldrich), $Ni(NO_3)_2$-$6H_2O$ (Sigma Aldrich), and $Al(NO_3)_3$-$9H_2O$ (98+%, Sigma Aldrich) were dissolved in a minimum amount of distilled water. A glycine to nitrate ratio of 0.5 was used in this study and a slight (5%) excess of lithium was included to accommodate lithium loss during synthesis. The resulting solutions were dehydrated on a hot plate in a stainless steel vessel until auto-ignition occurred. The resulting powders were collected, planetary balled milled for one hour in acetone, and dried under flowing nitrogen before being fired at 800° C (4° C/min heating rate) for four hours in air.

Laminate composite cathodes comprised of 84% active material, 8 % poly(vinylidine fluoride) (PVDF, Kureha Chemical Ind. Co. Ltd.), 4 wt.% compressed acetylene black, and 4 wt.% SFG-6 synthetic flake graphite (Timcal Ltd., Graphites and Technologies) were applied to carbon coated current collectors (Intelicoat Technologies) by automated doctor blade. 1.8 cm^2 electrodes having an average loading of 7-10 mg/cm^2 of active material were punched out. Coin cells (2032) were assembled in a helium filled glove box with a lithium metal anode and 1M $LiPF_6$ in 1:2 ethylene carbonate/dimethyl carbonate (EC/DMC) electrolyte solution (Ferro). Galvanostatic cycling was carried out on an Arbin BT/HSP-2043 cycler between limits of 2.0 and 4.3-4.7V. All cells were charged at a current density of 0.1 mA/cm^2 independent of the discharge rate.

Powder X-ray diffraction (XRD) was performed on a Phillips X'Pert diffractometer with an X'celerator detector using Cu Kα radiation to determine phase purity. A back loading powder holder was used to minimize the impact of any preferred orientation. Unit cell parameters were obtained from the patterns using the software package FullProf ([13]). Particle morphology was examined using transmission electron microscopy (TEM) on a Phillips CM200FEG (field emission gun) at an accelerating voltage of 200 kV. To prepare samples for TEM, powders were ground in a mortar and pestle under acetone and transferred to a holey carbon grid.

Results and Discussion

All materials were found to be phase pure by XRD powder diffraction (Figure 1) and can be indexed in the R-3m space group for all values of y in $LiNi_{0.4}Co_{0.2-y}Al_yMn_{0.4}O_2$. The clear separation of the 018 and 110 peaks reveal the high degree of lamellar character of the materials. The distinct absence of any γ-$LiAlO_2$ impurities even at high y values indicates that a completely cobalt free solid solution material can be readily synthesized. In contrast, it is not possible to make single-phase $LiNi_{1/3}Al_{1/3}Mn_{1/3}O_2$ where Co is fully replaced with Al ([14,15]).

Figure 2 shows the effect of Al substitution on the lattice parameters. Increasing Al content causes a decrease in the a parameter and a slight increase in the c parameter, leading to a minor decrease in the unit cell volume.
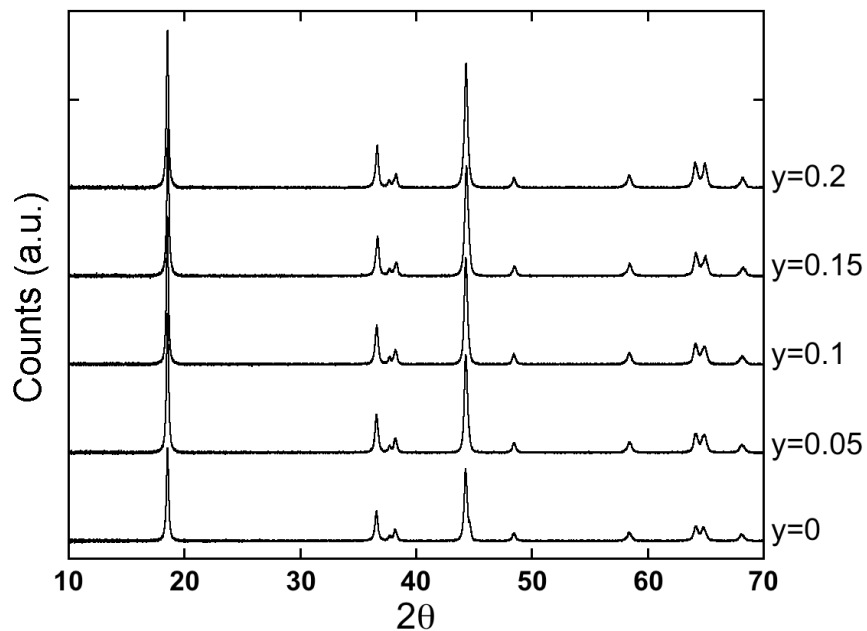

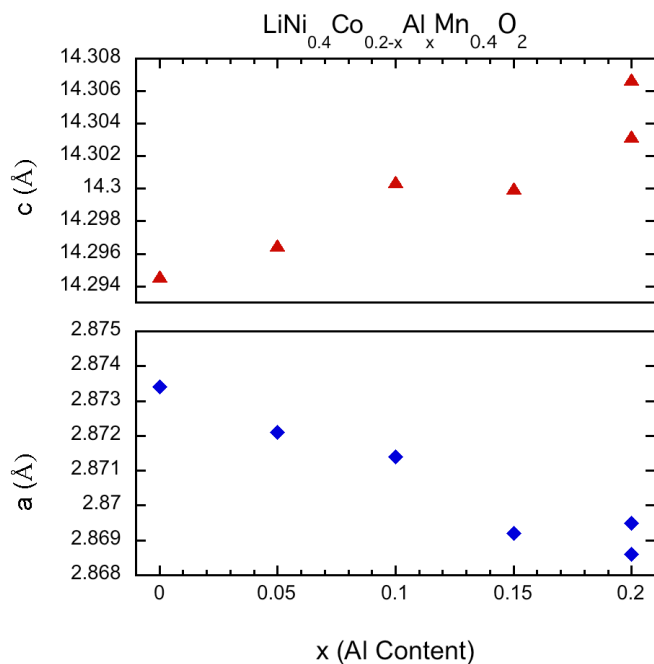Figure 1. Powder XRD patterns of the $LiNi_{0.4}Co_{0.2-y}Al_yMn_{0.4}O_2$ series.

Figure 2. Variation of the a and c lattice parameters with Al content in $LiNi_{0.4}Co_{0.2-y}Al_yMn_{0.4}O_2$.

The c/3a ratio can be taken as an indication of the degree of cation mixing. For a completely disordered structure with ideal cubic close packing (e.g., rock salt type), the

c/a ratio is 1.633 whereas, for a perfect layered structure with no ion-mixing such as LiTiS$_2$, the value is 1.793 (16). Figure 3 shows that c/3a ratio increases slightly as Al content is increased, implying that there is slightly less cation mixing. However, all values are intermediate between those found for rock salt and ideal layered structures, implying that some nickel ions may still be located in the van der Waals gaps.
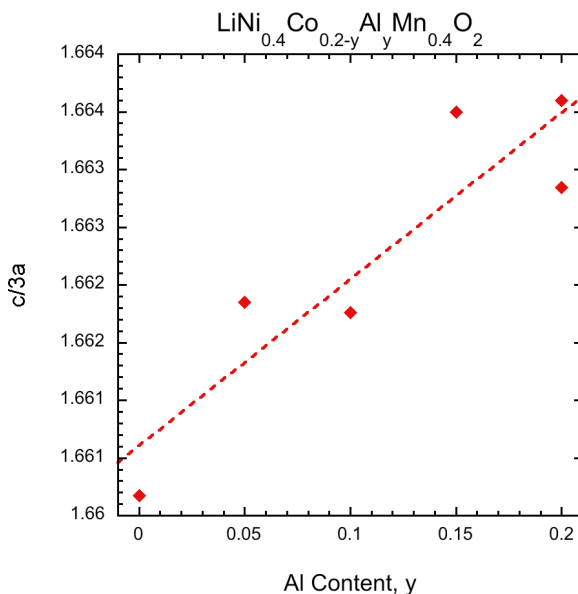

Figure 3. Variation of the c/3a ratio with y for the LiNi$_{0.4}$Co$_{0.2-y}$Al$_y$Mn$_{0.4}$O$_2$ series.

Powders made by the glycine-nitrate combustion method are composed of small primary particles approximately 50 nm in diameter, with varying degrees of agglomeration (Figure 4). Al substitution does not appreciably change the particle morphology.

Figure 5 shows differential capacity plots for Li/LiNi$_{0.4}$Co$_{0.2-y}$Al$_y$Mn$_{0.4}$O$_2$ (0≤y≤0.2) cells charged and discharged at 0.1 mA/cm^2 between 2.0 and 4.3V. These results reveal that there is a progressive shifting of the peak potentials to higher values as the Al content is increased. This may account for the observed decrease in capacity as y increases (Figure 6), for cells cycled between 2.0 and 4.3V. Although little Co is expected to undergo redox in this potential range, the low cutoff prevents full utilization because more capacity is shifted to a higher potential. Raising the upper voltage limit results in higher utilization initially for these electrodes but capacity fading is increased, possibly due to electrolyte oxidation. The best results in this voltage range were obtained for the composition y=0.05. The low Al substitution has an insignificant impact on the specific capacity obtained and the cycling behavior is marginally improved, so that, by the 15th cycle, the LiNi$_{0.4}$Co$_{0.15}$Al$_{0.05}$Mn$_{0.4}$O$_2$ electrode outperforms the unsubstituted material.
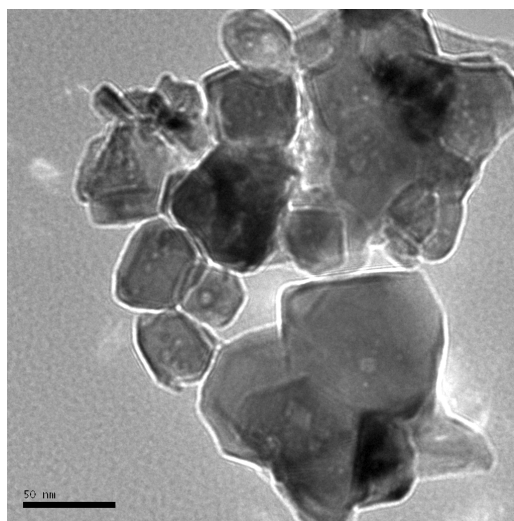
Figure 4. TEM image of $LiNi_{0.4}Co_{0.2}Mn_{0.4}O_2$.

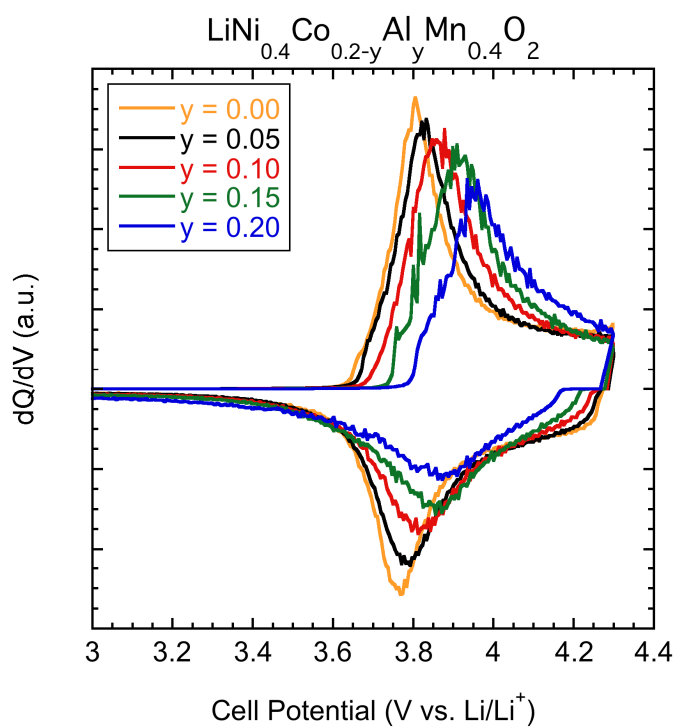Figure 5. Differential capacity plots (first cycles) for $Li/LiNi_{0.4}Co_{0.2-y}Al_yMn_{0.4}O_2$ $(0 \leq y \leq 0.2)$ cells charged and discharged galvanostatically at 0.1 mA/cm^2.
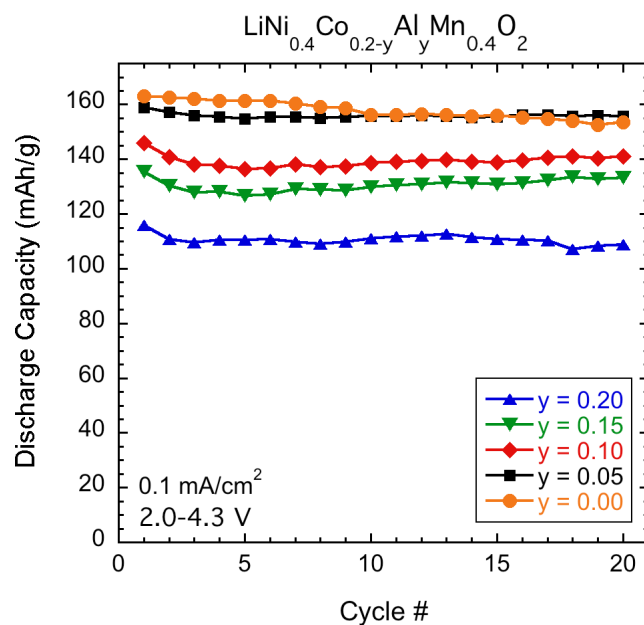
Figure 6. Discharge capacity as a function of cycle number for Li/LiNi$_{0.4}$Co$_{0.2-y}$Al$_y$Mn$_{0.4}$O$_2$ cells cycled at 0.1 mA/cm^2 between 2.0 and 4.3V.
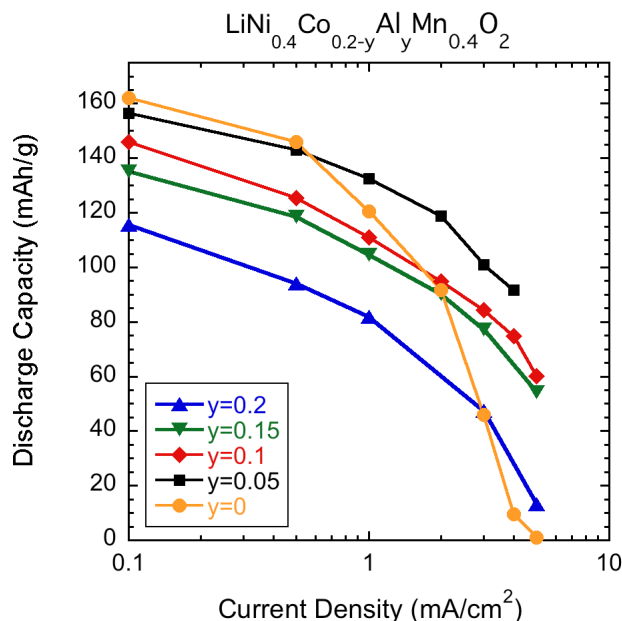

Figure 7. Discharge capacity between 4.3 and 2.0V as a function of current density for Li/LiNi$_{0.4}$Co$_{0.2-y}$Al$_y$Mn$_{0.4}$O$_2$ (0≤y≤0.2) cells

Figure 7 shows the rate capabilities of Li/LiNi$_{0.4}$Co$_{0.2-y}$Al$_y$Mn$_{0.4}$O$_2$ (0≤y≤0.2) cells discharged between 4.3 and 2.0V. All Al-substituted materials outperform the parent compound above certain critical current densities, which vary with the value of y. LiNi$_{0.4}$Co$_{0.15}$Al$_{0.05}$Mn$_{0.4}$O$_2$ is clearly superior to LiNi$_{0.4}$Co$_{0.2}$Mn$_{0.4}$O$_2$ at all current densities above 0.5 mA/cm^2, and still delivers over 100 mAh/g at 5 mA/cm^2 whereas LiNi$_{0.4}$Co$_{0.2}$Mn$_{0.4}$O$_2$ cannot be discharged at all. Inspection of the discharge profiles indicates that cell polarization for the Al-substituted materials is much less than for the

parent $LiNi_{0.4}Co_{0.15}Al_{0.05}Mn_{0.4}O_2$. The origins of the rate enhancement induced by the Al substitution are currently under investigation.

Summary

It has been shown that phase-pure materials having the compositions $LiNi_{0.4}Co_{0.2-y}Al_yMn_{0.4}O_2$ ($0 \leq y \leq 0.2$) can be prepared readily using the glycine-nitrate combustion synthesis method. Al substitution decreases the unit cell volumes slightly and results in marginally less ion-mixing, without substantially affecting the particle morphology. Although specific capacity in lithium cells between 4.3 and 2.0V is reduced in proportion to the amount of Al substitution in the materials, rate capability is enhanced considerably. The best-performing material has a composition of $LiNi_{0.4}Co_{0.15}Al_{0.05}Mn_{0.4}O_2$, which delivers 160 mAh/g at 0.1 mA/cm^2 and 100 mAh/g at 5 mA/cm^2.

Acknowledgments

References

1. S. Patoux and M. M. Doeff, *Electrochem. Commun.*, **6**, 767 (2004).
2. B. J. Hwang, Y. W. Tsai, D. Carlier and G. Ceder, *Chem. Mat.*, **15**, 3676 (2003).
3. M. Ma, N. A. Chernova, B. H. Toby, P. Y. Zavalij and M. S. Whittingham, *Journal of Power Sources*, **165**, 517 (2007).
4. S. Buta, D. Morgan, A. Van der Ven, M. K. Aydinol and G. Ceder, *J. Electrochem. Soc.*, **146**, 4335 (1999).
5. G. Ceder, Y. M. Chiang, D. R. Sadoway, M. K. Aydinol, Y. I. Jang and B. Huang, *Nature*, **392**, 694 (1998).
6. M. K. Aydinol, A. F. Kohan, G. Ceder, K. Cho and J. Joannopoulos, *Phys. Rev. B*, **56**, 1354 (1997).
7. Y. I. Jang, B. Y. Huang, H. F. Wang, G. R. Maskaly, G. Ceder, D. R. Sadoway, Y. M. Chiang, H. Liu and H. Tamura, *Journal of Power Sources*, **82**, 589 (1999).
8. C. Julien, G. A. Nazri and A. Rougier, *Solid State Ionics*, **135**, 121 (2000).
9. Q. Zhong and U. von Sacken, *J. Power Sources*, **-54**, 221 (1995).
10. T. Ohzuku, T. Yanagawa, M. Kouguchi and A. Ueda, *Journal of Power Sources*, **68**, 131 (1997).
11. T. Ohzuku, A. Ueda and M. Kouguchi, *J. Electrochem. Soc.*, **142**, 4033 (1995).
12. L. A. Chick, L. R. Pederson, G. D. Maupin, J. L. Bates, L. E. Thomas and G. J. Exarhos, *Materials Letters*, **10**, 6 (1990).
13. J. Rodriguez-Carvajal, *Physica B: Condensed Mater*, **192**, 55 (1993).
14. J. D. Wilcox, S. Patoux, and M. M. Doeff, unpublished results.
15. S.-K. Hu, T.-C. Chou, B.-J. Hwang and G. Ceder, *Journal of Power Sources*, **160**, 1287 (2006).
16. J. K. Ngala, N. A. Chernova, M. Ma, M. Mamak, P. Y. Zavalij and M. S. Whittingham, *Journal of Materials Chemistry*, **14**, 214 (2004).